SLAC-PUB-10314
January 2004

Results of the VISA SASE FEL Experiment at 840 nm

A. Murokh[a,*], R. Agustsson[a], M. Babzien[b], I. Ben-Zvi[b], L. Bertolini[c], K. van Bibber[c], R. Carr[d], M. Cornacchia[d], P. Frigola[a], J. Hill[c], E. Johnson[b], L. Klaisner[d], G. Le Sage[c], M. Libkind[c], R. Malone[b], H-D. Nuhn[d], C. Pellegrini[a], S. Reiche[a], G. Rakowsky[b], J. Rosenzweig[a], R. Ruland[d], J. Skaritka[b], A. Toor[c], A. Tremaine[c], X. Wang[b], V. Yakimenko[b]

[a] *UCLA - Department of Physics and Astronomy, 405 Hilgard Ave., Los Angeles, CA 90095-1547, USA*
[b] *Brookhaven National Laboratory, Upton, NY 11973, USA*
[c] *Lawrence Livermore National Laboratory, Livermore, CA 94551, USA*
[d] *Stanford Linear Accelerator Center, Stanford, CA 94309, USA*

Abstract

VISA (Visible to Infrared SASE Amplifier) is a high-gain self-amplified spontaneous emission FEL, which achieved saturation at 840 nm within a single-pass 4-m undulator. A gain length shorter than 18 cm has been obtained, yielding the gain of 2×10^8 at saturation. The FEL performance, including spectral, angular, and statistical properties of SASE radiation, has been characterized for different electron beam conditions. The results are compared to 3-D SASE FEL theory and start-to-end numerical simulations of the entire injector, transport, and FEL system. Detailed agreement between simulations and experimental results is obtained over the wide range of the electron beam parameters.

1. Introduction and Experimental Setup

The concept of an unseeded, single pass, self-amplified spontaneous emission free-electron laser (SASE-FEL) was introduced in the early 80s [1,2]. More recently, a series of successful experiments demonstrated high gain SASE operation, and established agreement between the main elements of the theory and experiments, in the IR [3], visible [4], and ultraviolet [5] spectral ranges. These results have led to the design of the Linac Coherent Light Source (LCLS) X-ray FEL project at SLAC [6] and a similar project at DESY. With 10 GW peak power and sub-picosecond pulse length, LCLS will significantly enhance our research capabilities at the molecular and atomic level. The VISA SASE-FEL project [7], reported here, was designed to achieve high gain and saturation in a short undulator, in the regime directly scalable to future LCLS operation.

VISA reached saturation in 3.6-3.8 m at 840 nm, with a gain length by a factor of 3 shorter than previously achieved in this spectral range. Such results were made possible by implementing a novel

* *E-mail address:* murokh@physics.ucla.edu

Work supported in part by the Department of Energy contract DE-AC03-76SF00515.

Presented at the 24th International Free Electron Laser Conference and 9th FEL r Users Workshop (FEL 2002), 9/9/2002 - 9/13/2002, Argonne, IL, USA

undulator design, optimized for the low emittance electron beam produced at the Accelerator Test Facility (ATF) [8]. The focus of this work is on the results obtained at the fundamental wavelength, while other measurements including FEL harmonics and microbunching are reported elsewhere [9].

The ATF injector consists of a 1.6-cell S-band photocathode gun and two consecutive SLAC-type linac structures that accelerate the beam to near 71 MeV [10]. A 20° double-bend transport section (dogleg) directs the beam towards the VISA in-vacuum undulator [11] – a Halbach array of 220 periods, each 1.8 cm long. The undulator pole magnets generate an on-axis peak field of 0.75 T. In addition, a periodic quadrupole lattice provides intra-undulator strong focusing to reduce the average electron beam β-function to 30 cm in both planes. Magnets alignment and shimming, performed at BNL in tandem with the pulsed-wire measurements [12], provide a desired central trajectory straightness of better than 100 μm [13] throughout each sequential pair of 4 individual undulator segments, supported independently from the vacuum chamber [14]. To co-align the magnetic axis of *all* 4 segments, an interferometric alignment procedure [15] was implemented. Motion of the undulator segments is monitored optically with an accuracy of 10-μm [16].

The undulator design includes 8 diagnostic ports, spaced 50 cm apart, to measure SASE properties along the undulator length and to characterize the electron beam position and profile at three points per betatron period. When a diagnostic probe intercepts a beam path, the active area of the probe – a double-sided silicon mirror – can be positioned to either reflect FEL light towards SASE diagnostics, or to generate OTR for imaging of the electron beam [17].

Table 1: Electron beam characteristics and SASE FEL properties measured without compression (A) and with compression (B).

	Case A	Case B
Electron Beam Energy	71.2 MeV	70.7 MeV
Beam Charge, Q	250 pC	140 pC
Horizontal Emittance, ε_n	2.1±0.2 μm	3.3±0.2 μm
Peak Current, I_p	55 Amp	250 Amp
RMS Energy Spread, σ_γ/γ	< 0.10 %	0.17 %
FEL Gain Length, L_g	29.7 cm	17.9 cm
SASE Wavelength, λ_r	831 nm	842 nm
# of Temporal Spikes, M	4-5	1-2

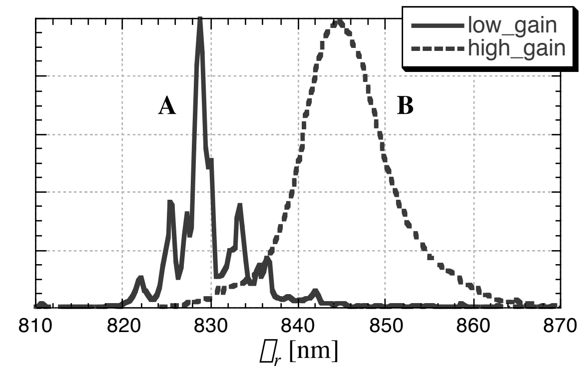

Fig. 1. Comparison of SASE radiation spectra measured without (A) and with (B) compression. The spiky structure in Case A indicates many longitudinal modes (i.e. longer bunch length).

2. Results and Analysis

Electron beam characterization was initially performed at the linac exit (Table 1A). The projected emittance, ε_n, was determined with a quadrupole scanning technique; and to evaluate the beam current a linear chirp was applied to the beam in the linac, mapping a longitudinal particles distribution to the horizontal profile measured around the bend. With a normalized emittance of 2.1 μm and a peak current of 55 Amp, a SASE gain of G $\approx 7\times10^4$ was initially obtained at 830 nm. Corresponding SASE spectral measurements, shown in Figure 1A, indicate a multi-spike temporal profile of SASE with the lasing core of the electron beam typically about 500 μm long [7].

Further studies, however, showed that much stronger SASE gain and saturation can be achieved by changing the beam optics in the dogleg and detuning the linac RF phase. This optimized gain condition was accompanied by changes in the SASE radiation spectra, where the spiky structure was replaced with a smooth peak (Fig. 1B), pointing towards the shorter bunch length [18]. Based on these observations, and beamline simulations, the FEL performance improvement was attributed to a non-linear peak current enhancement in the dispersive section of the beamline [19]. With new beamline optics, the linac phase detuning generated positive R_{56} of the dispersive section (by reducing the beam energy), and induced energy chirping in the electron beam, causing the bunch compression.

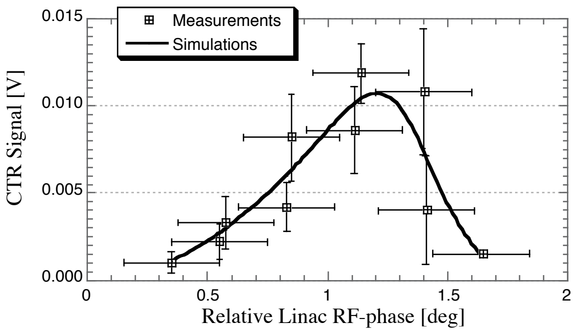

Fig. 2. Measured CTR signal intensity exhibits a sharp peak within a narrow window (~ 1.5°) of the linac RF phase.

To experimentally verify the bunch compression hypothesis, a coherent transition radiation (CTR) diagnostic was implemented. The intensity of the CTR signal is inversely proportional to the beam RMS bunch length σ_z. The signal, generated by a 45°-mirror intersecting the beam path *after* the dispersive section, is directed into a far-infrared bolometer. The CTR intensity (Fig. 2) shows a strong correlation with the linac RF phase, which is an evidence of bunch compression. In addition, an insertable low-pass filter with a known frequency roll-off was used for quantitative assessment of the high frequency CTR component. Measurements with and without the filter provide a benchmark for the numerical modelling of the system. As a result, it was shown that the electron beam indeed was a subject to strong compression in the dispersive section, yielding a peak current up to 250 A, giving a dramatic improvement of SASE gain (Table 1B).

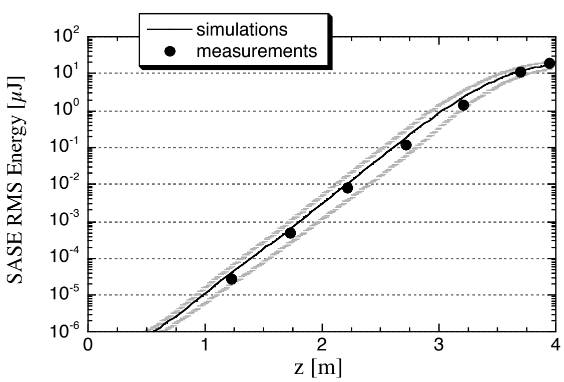

Fig. 3. Measured SASE evolution along the undulator length and numerical simulations (grey lines are the RMS boundaries of the set of GENESIS runs). The amplification curve yields power gain lengths of 17.9 cm and saturates near the undulator exit.

The photon beam from any of 8 diagnostic ports can be directed into the joulemeter. The measured SASE radiation intensity noticeably exceeds broadband spontaneous emission starting from the diagnostic port 3 (1.25 m into the undulator). Due to the sensitivity of the compression process to small changes in the linac RF phase, the FEL intensity fluctuations are generally dominated by the RF jitter. However, a beam collimator in the dispersive section allowed correlation of the linac phase to the charge transmission through the dogleg [20]. Hence, by applying charge selection criterion to the multi-shot data sets, one can both, reduce linac noise to extract SASE statistical properties, and be systematic in comparing data sets obtained at different locations.

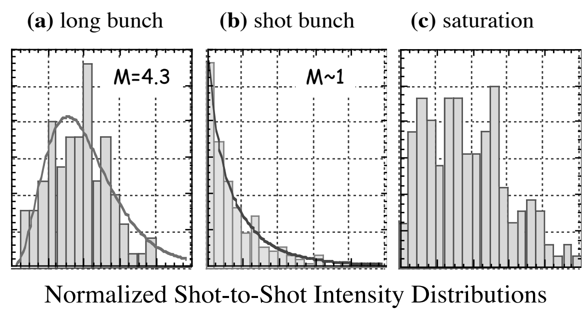

Fig. 4. SASE fluctuations (a) without compression, and at high gain measured (b) inside the undulator and (c) at the undulator exit.

The gain curve in Figure 3 shows the SASE intensity evolution along the undulator length. The fit to the exponential part of the curve yields a power gain length of 17.9 cm, corresponding to 3-D FEL parameter $\rho \approx 0.0046$, reduced from 1-D limit by a factor of $(1+\eta) \approx 1.75$, mostly due to diffraction. Near the undulator exit, the curve deviates from the exponential behaviour, indicating saturation. Further evidence of saturation is found in the statistical properties of the SASE signal (Fig. 4). When there is no compression (a), a Γ-function fit [21] indicates 4-5 temporal spikes (consistent with the spectrum in Fig. 1A). With the compressed beam, a distribution inside the undulator (b) resembles a negative exponential, characteristic of a single spike (mode) lasing. At the undulator exit, however, the distribution changes (**c**) – being dominated by the shot-to-shot fluctuations in the saturation length, that are significant for short bunches [18].

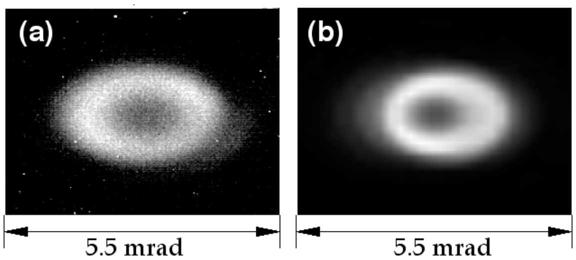

Fig. 5. Far field angular distribution of SASE radiation (a) measured on the CCD camera, and (b) simulated with GENESIS.

For the measured ρ, saturation is also expected from the theoretical estimate of the FEL saturation length [22], $L_{sat} \approx \lambda_u / \rho = 3.9$ m. The measured bandwidth, $(\Delta\omega/\omega)_f \approx 1.2$ %, also agrees to the value expected from theory, if one includes the contribution of the beam chirp $\Delta\omega/\omega \approx 2\rho \cdot (1 + 2(\Delta\gamma/\gamma\rho)^2)$. Finally, SASE power at saturation is about 75 MW, consistent with 3-D scaling $P_{sat} \sim P_{beam}\rho$. The final state SASE gain $G \equiv (dP/d\omega)_f/(dP/d\omega)_{noise}$ is evaluated based on the treatment given in [23]:

$$G^{-1} \approx \frac{3\rho}{4}\left(\frac{K^2[JJ]^2}{1+K^2/2}\right)\frac{I_b}{I_A}\frac{m_e c^2}{P_f / k_r c}\left(\frac{\Delta\omega}{\omega}\right)_f \frac{\tilde{L}_g}{\lambda_u}.$$

With $K = 1.26$, and an average beam current over the spike length $I_b = 210$ A, the gain value is $G \approx 2 \times 10^8$.

Nonlinear effects during the transport of the electron beam became critical for understanding SASE properties, and simulations of the entire experiment were required to model the FEL results. PARMELA was used to model acceleration through the gun and linac sections and match post-linac beam measurements (Table 1), followed by running the code ELEGANT [24] to simulate bunch compression in the dogleg, including the effects of coherent synchrotron radiation (CSR). ELEGANT runs show that the emittance growth in the bends due to CSR is small, $\Delta\varepsilon_n^{CSR} < 0.3$ µm; however, at the point of maximum compression, an effective horizontal slice emittance increases up to $\varepsilon_n^{eff} \approx 3.5$ µm due to the 2nd order dispersion. Once the PARMELA-ELEGANT model had fully reproduced the CTR measurements (Fig. 2) its output was converted into the input file for GENESIS 1.3 [25]. The FEL simulations show an excellent agreement with the measured SASE gain evolution (Fig. 4), as well as spectral and angular properties of the radiation. Figure 5 displays the measured angular profile of SASE intensity along with the far field distribution from the GENESIS output. The hollow profile of the SASE radiation cone, repeatedly observed experimentally, is linked to the strong asymmetry in the energy-correlated horizontal phase space distribution, after the bunch compression. Having this unusual result reproduced with GENESIS indicated a new level of insight into the dynamics of the electron beam and SASE FEL systems, obtained by synthesis of copious diagnostic measurements and rigorous, detailed simulations.

This work is done under the DOE contract No DE-FG03-92ER40693.

3. References

[1] R. Bonifacio, C. Pellegrini, and L. Narducci, Opt. Commun. **50**, 373 (1984).
[2] A.M. Kondratenko, E.L. Saldin, Part. Accel. **10**, 207 (1980).
[3] M. Hogan *et al.*, Phys. Rev. Lett. **81**, 4867 (1998).
[4] S.V. Milton *et al.*, Science **292**, 2037 (2001).
[5] V. Ayvazyan *et al.*, Phys. Rev. Lett. **88**, 104802 (2002).
[6] LCLS Design Study Report, SLAC-R-521 (1998).
[7] A. Murokh, Ph.D. thesis, UCLA (2002).
[8] X. Wang *et al.*, Phys. Rev. E **54**, 3121 (1996).
[9] A. Tremaine *et al.*, Phys. Rev. Lett. **88**, 204801 (2002); these proceedings.
[10] X. Wang *et al.*, Prs. PAC 99, 3495 (1999).
[11] R. Carr *et al.*, Phys. Rev. STAB **4**, 122402 (2001).
[12] G. Rakowsky *et al.*, Prs. PAC 99, 2698 (1999).
[13] P. Emma, H.D. Nuhn, Prs. FEL 98 **II**, 35 (1999).
[14] M. Libkind *et al.*, Prs. PAC 99, 2477 (1999).
[15] R. Ruland *et al.*, Prs. PAC 99, 1390 (1999).
[16] A. Tremaine, A. Murokh, and X.J. Wang, BNL Report No. 68170, 2001 (unpublished).
[17] A. Murokh *et al.*, Prs. FEL 99, **II**, 35 (2000).
[18] R. Bonifacio *et al.*, Phys. Rev. Lett. **73**, 70 (1994).
[19] J.B. Rosenzweig, (private communication).
[20] A. Murokh *et al.*, Prs. PAC 2001, 2748 (2001).
[21] E.L. Saldin *et al.*, Opt. Comm. **148,** 383 (1998).
[22] K.J. Kim, Phys. Rev. Lett. **57**, 1871 (1986).
[23] L.H. Yu and S. Krinsky, Nucl. Instr. Meth. A **285,** 119 (1989).
[24] M. Borland, (private communication).
[25] S. Reiche, Nucl. Instr. Meth. A **429,** 243 (1999).